HETEROCYCLES, Vol. 100, No. 11, 2020, pp. 1799 - 1815. © 2020 The Japan Institute of Heterocyclic Chemistry
Received, 9th July, 2020, Accepted, 2nd September, 2020, Published online, 9th September, 2020
DOI: 10.3987/COM-20-14317

SYNTHESIS AND EVALUATION OF β-GALACTOSIDASE-TARGETING SPIN-LABEL PROBE: 5-*O*-β-D-GALACTOSYL-5-HYDROXY-1,1,3,3-TETRAMETHYLISOINDOLINE-2-OXYL

Koya Sugawara, Hiroyuki Konno, Tomohiro Ito, and Shingo Sato*

Graduate School of Science and Engineering, Yamagata University, Jonan 4-3-16, Yonezawa-shi, Yamagata 992-8510, Japan. E-Mail: shingo.s0623@gmail.com

Abstract – In this study, 3-hydroxymethyl-2,2,5,5-tetramethylpyrrolidine-1-oxyl, 4-hydroxy-2,2,6,6-tetramethylpiperidine-1-oxyl, and 5-hydroxy-1,1,3,3-tetramethylisoindoline-2-oxyl *O*-galactosides (PG, TG, and IG) were synthesized. Moreover, their reduction reactivity (RR) for ascorbic acid and hydrolysis reactivity (HR) for *β*-galactosidase were measured via electron paramagnetic resonance (EPR) spectroscopy and high-performance liquid chromatography (HPLC), respectively. The both rate constants for these two reactions were found to exhibit the following order: RR: TG > IG > PG, and HR: IG > PG > TG. Based on the results of the in vitro assay, IG was selected as the candidate for the bioassay. The bioassay of IG by HeLa cells (cancer cells) and PC12 cells (normal cells) indicated that after 20 min of IG addition, more nitroxide radicals were located in the cancer cells than in the normal cells, while their EPR intensity was low.

INTRODUCTION

Recently numerous studies on the staining of specific cells by fluorescent dyes have been conducted.[1-3] Urano et al. reported that a *β*-galactosylfluorescein analog was specifically recognized by cancer cells, subsequently hydrolyzed by *β*-galactosidase, and finally emitted fluorescence. Moreover, this analog was employed in practical applications wherein small cancer cells remaining after injuries were identified via the emission on spraying *β*-galactosylfluorescein, thereby enabling their efficient removal.[4,5] Concurrently, nitroxide radicals have been studied as non-invasive EPR-visualized spin-label probes.[6-9] If this method is applied to the detection of cancer cells, non-invasive detection of the cancer cells would be possible.

We have explored new nitroxide-radical hybrid compounds, such as glucose–nitroxide,[10] fluorophore–nitroxide,[11,12] and drug–nitroxide[13-15] compounds, as a spin-label probe to explore redox states *in vivo*. We succeeded in EPR-imaging of the anti-inflammatory effect in septic mouse brain by ibuprofen-PROXYL hybrid-compound.[13] Bottle and coworkers reported that indomethacin-TEMPOL hybrid-compound displayed not only anti-oxidant and anti-inflammatory effects but also anti-cancer activity for lung cancer cells.[16] Based on the above research we have been studied nitroxide *O*-*β*-galactoside as a non-invasive EPR-visualizable spin-label probe for cancer cells, which we discuss below.

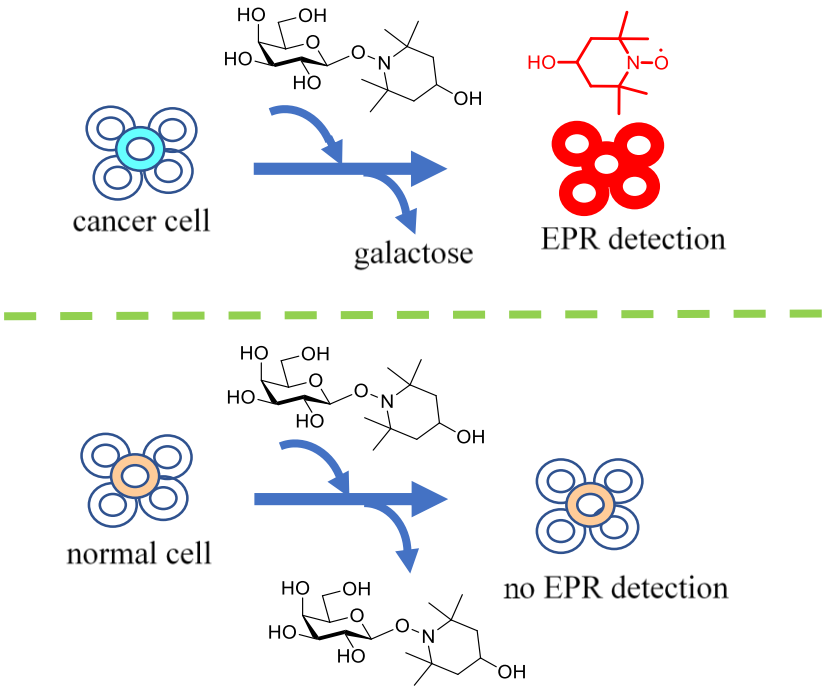

Figure 1. Proposal I for the EPR detection of the cancer cells by nitroxide *O*-*β*-galactoside selective digestion

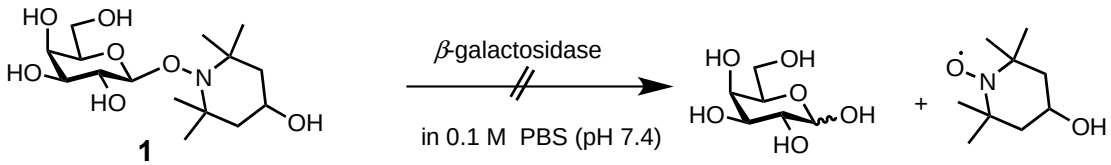

Scheme 1. Trial of hydrolysis of **1** by *β*-galactosidase

First, we considered and tested hydroxylamine *O*-*β*-galactoside **1**[17] for its selective hydrolysis by the more active *β*-galactosidase, followed by oxidiation in cancer cells compared to that in normal cells, to generate EPR-detectable nitroxide radicals (Proposal I, Figure 1). However, **1** was difficult to hydrolyze

because of the bulkiness of its tetra-methyl groups (Scheme 1). Next, we planned new nitroxide radical *O*-*β*-galactosides as a spin-label probe, which are not a non-radical like **1** but expect to be selectively recognized by cancer cells and hydrolyzed by *β*-galactosidase, affording more hydrophobic and longer duration nitroxide radicals than their glycoside (proposal II, Figure 2). Since the reactivity of our synthetic nitroxide-hybrid compounds such as fluorescent nitroxides, glucosyl nitroxides, nitroxide-drugs and each nitroxide for L-ascorbic acid (AsA) was all same or the latter was a little bit fast, it is considered that the reactivity of galactoside and its aglycone for AsA in this work is also analogous.

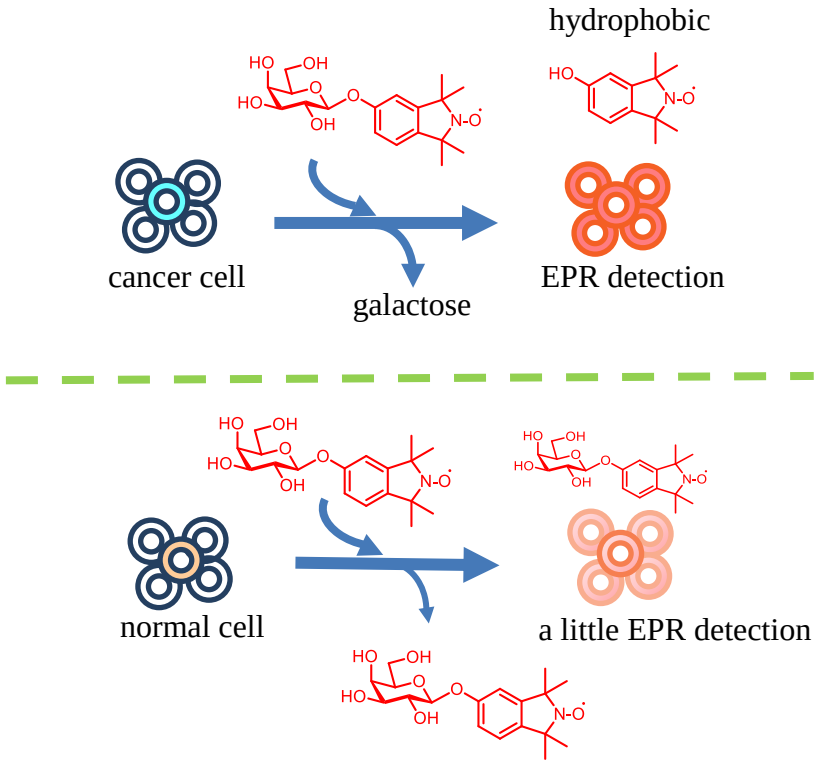

Figure 2. Proposal II for the EPR detection of the cancer cells by nitroxide *O*-*β*-galactoside selective digestion

Motivated by the above concept, in study, we suggested three candidate, nitroxide *O*-*β*-galactosides as spin-label probes: *O*-*β*-D-galactosyl-3-hydroxymethyl-2,2,5,5-tetramethylpyrrolidine-1-oxyl (*O*-*β*-D-galactosyl PROXYL **2**), *O*-*β*-D-galactosyl-4-hydroxy-2,2,6,6-tetramethylpiperidine-1-oxyl (4-*O*-*β*-D-galactosyl TEMPO **3**), and *O*-*β*-D-galactosyl-5-hydroxy-1,1,3,3-tetramethylisoindoline-2-oxyl (5-*O*-*β*-D-galactosyl HTMIO **4**). It was characterized that **2** possesses a primary alcohol and a five-membered ring nitroxide, **3** comprises a secondary alcohol and a six-membered ring nitroxide, and **4** includes a phenol-hydroxyl and a benzene-ring condensed five-membered ring nitroxide (Figure 3).

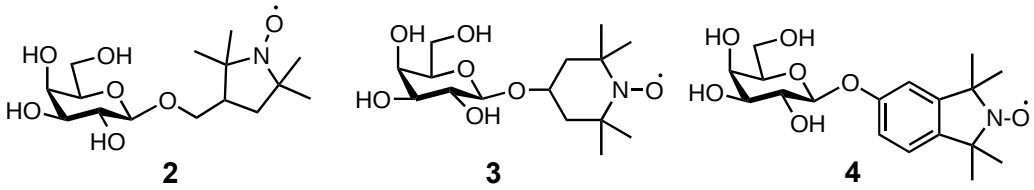

Figure 3. *O*-β-D-galactosyl PROXYL (**2**), TEMPO (**3**), and HTMIO (**4**)

RESULTS AND DISCUSSION

Synthesis

In this study, 3-hydroxymethyl PROXYL (**5**) and 4-hydroxy-TEMPO (**6**) were synthesized by conventional methods,[18-20] and 5-hydroxy-TMIO (**7**) was prepared by according to the method established by Bottle et al.[21-25]

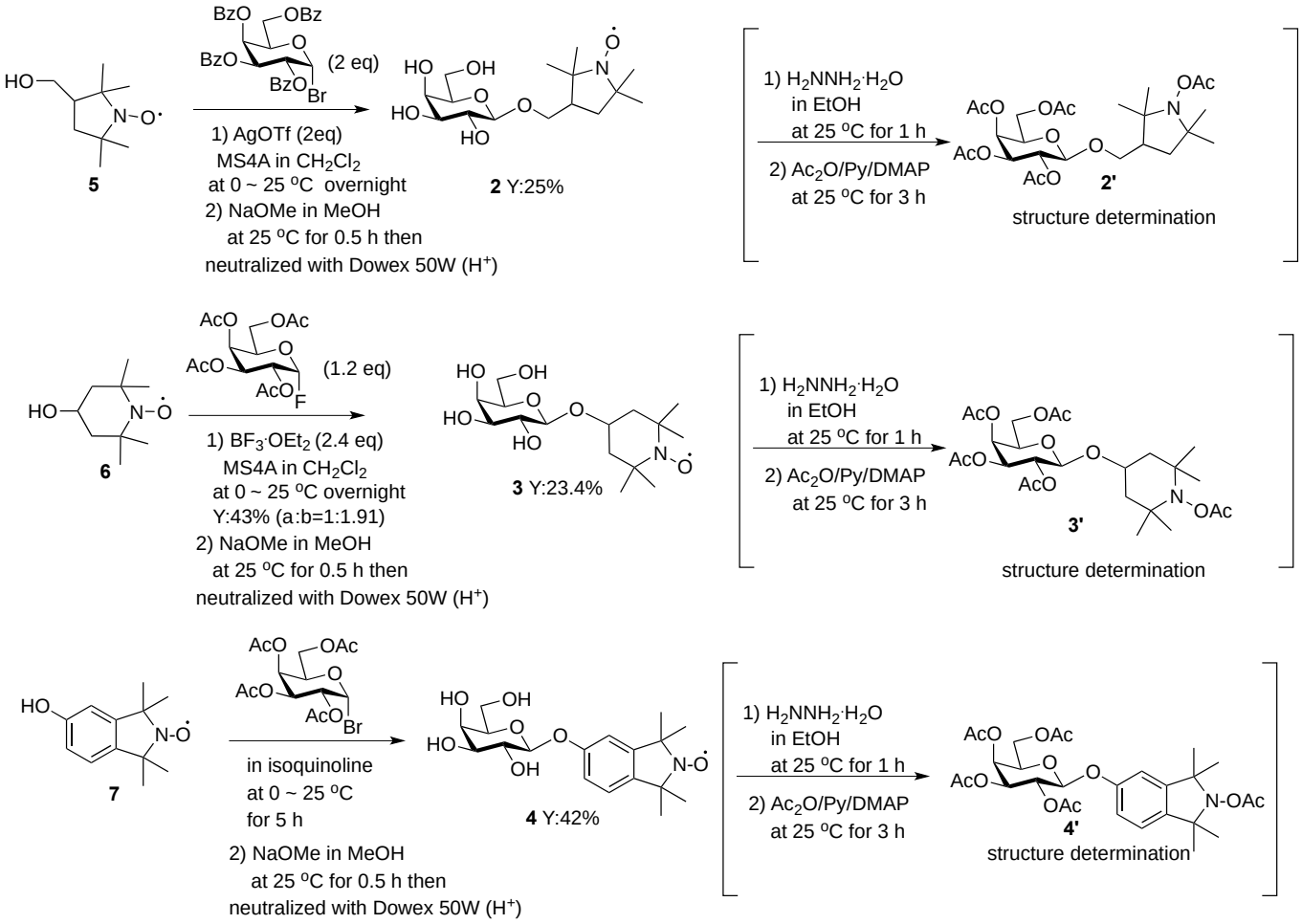

Scheme 2. Synthesis of *O*-β-D-galactosyl nitroxide-radicals **2**, **3**, and **4**

These three nitroxide-radical *O*-*β*-D-galactosides were synthesized as follows: *O*-*β*-D-galactosyl PROXYL **2** was synthesized by the glycosylation of **5** with 2 eq. bulky per-*O*-benzoyl-*α*-D-galactosyl bromide in the presence of 2 eq. silver trifluoromethanesulfonate (AgOTf). This was followed by de-*O*-benzoylation with sodium methoxide (NaOMe), to obtain **2** exclusively with 25% yield. Subsequently, 4-*O*-*β*-D-galactosyl TEMPO **3** was synthesized by the glycosylation of **6** with 2.4 eq. per-*O*-acetyl-*α*-D-glactosyl fluoride in the presence of 2.4 eq. trifluoroborane diethyl ether complex ($BF_3 \cdot OEt_2$). This was followed by de-*O*-acetylation with NaOMe, to afford **3** *β*-selectively with 28% yield. Next, 5-*O*-*β*-D-galactosyl HTMIO **4** was synthesized by the glycosylation of **7** with per-*O*-acetyl-*α*-D-galactosyl bromide in isoquinoline.[26-28] This was followed by de-*O*-acetylation with NaOMe, to afford **4** exclusively with 42% yield. The structure of each nitroxide-radical *O*-*β*-D-galactoside was identified via nuclear magnetic resonance (NMR) analysis of the hydroxylamine acetate obtained by the hydrazine reduction of the corresponding nitroxide radical followed by acetylation (Scheme 2).

Measurements

The three synthesized nitroxide *O*-galactosides were evaluated by the reduction with AsA, the typical reducing substance in the living body and the hydrolysis with *β*-galactosidase.

Reduction rate constants *k* ($M^{-1}s^{-1}$) under 50-fold excess ascorbic acid

The rates of reduction of nitroxides **2**–**4** were studied under pseudo-first-order conditions using a 50-fold excess of AsA in 0.1 M phosphate buffer solution (PBS) (pH 7.4). The second-order rate constants, *k* ($M^{-1}s^{-1}$), were obtained by monitoring the decay of the ratio of the lowest-field signal of the triplet signals of the nitroxides to a signal of the Mn marker from 1 min to 5 min after the reaction at 295 K (Figure 4, Table 1).[14,15] The decay of **2** and **4** due to reduction was stable, with high R^2 values of 0.99 and 0.98, respectively. However, the reduction of **3** was significantly low, with a low R^2 value of 0.81. The order of the decay due to reduction was **3** > **4** > **2**. The rate constant for **3** was 2.3 ± 0.4 $M^{-1}s^{-1}$, which is 2.4 times greater than that for **4** (0.95 ± 0.03), which was 2.6 times larger than that for **2** (0.37 ± 0.13). Each reduction rate constant of the three nitroxides kept a similar difference. As **2** was associated with a small rate constant and R^2, the rates of reduction for all the nitroxides were subsequently measured using a 100-fold excess of AsA in 0.1 M PBS (pH 7.4).

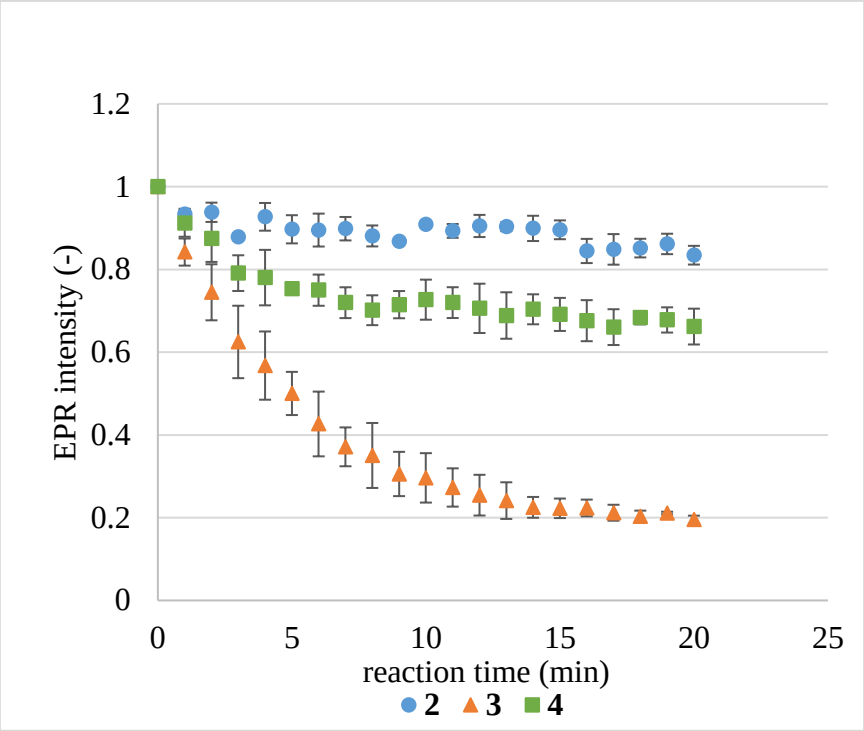

Figure 4. Time-dependent reduction profiles of the three nitroxide *O*-galactosides **2**–**4** with a 50-fold AsA in 0.1 M PBS (pH 7.4) at 295 K. Each data represents mean ± S.D., n = 3.

Table 1. Pseudo second-order rate constants k ($M^{-1}s^{-1}$) for the initial rates of reduction of the three nitroxide *O*-galactosides **2**–**4** with a 50-fold excess of AsA in 0.1 M PBS (pH 7.4) at 295 K, based on the Figure 4. (mean ± S.D., n = 3).

compound	k ($M^{-1}s^{-1}$)	R^2
2	0.37 ± 0.13	0.81
3	2.3 ± 0.36	0.99
4	0.95 ± 0.031	0.98

Reduction rate constants k ($M^{-1}s^{-1}$) under 100-fold excess AsA

In a 100-fold excess of AsA, the reduction rate constants for **2** and **4** presented suitable decay curves and high R^2 (0.99); in comparison, **3** was easily reduced, with low R^2 (0.96). The rate constant for **3** was 4.9 ± 0.3 $M^{-1}s^{-1}$ and 6.5 times larger than that of **4** (0.75 ± 0.02), which was 3.3 times larger than that for **2** (0.23 ± 0.08). Thus, the order of the reduction rate constants in the 100-fold excess AsA is the same as that in the 50-fold excess AsA (Figure 5, Table 2).

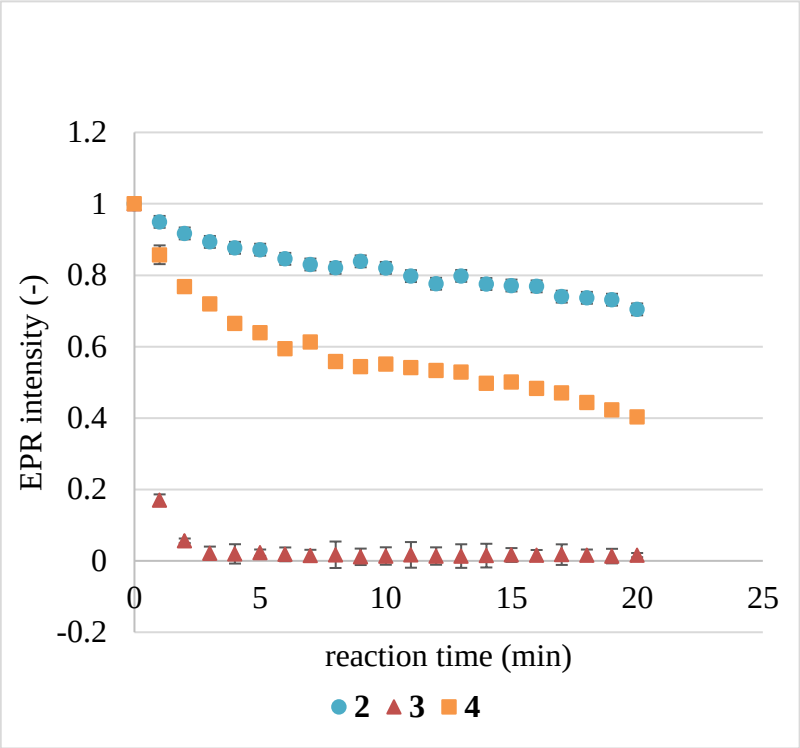

Figure 5. Time-dependent reduction profiles of the three nitroxide *O*-galactosides **2**–**4** with a 100-fold AsA in 0.1 M PBS (pH 7.4) at 295 K. Each data represents mean ± S.D., n = 3.

Table 2. Pseudo second-order rate constants k ($M^{-1}s^{-1}$) for the initial rates of hydrolysis of the three nitroxide *O*-galactosides **2**–**4** with a 100-fold excess of AsA at 295 K, based on the Figure 5. (mean ± S.D., n = 3).

compound	k ($M^{-1}s^{-1}$)	R^2
2	0.23 ± 0.075	0.99
3	4.9 ± 0.31	0.96
4	0.75 ± 0.023	0.99

Hydrolysis rate constants k (min^{-1}) for initial rates of hydrolysis of the three nitroxide *O*-*β*-D-galactosides 2–4 with 20 μL *β*-galactosidase

The rates of hydrolysis of nitroxide *O*-*β*-D-galactosides **2**–**4** were studied under pseudo-first-order conditions using 20 μL *β*-galactosidase in 0.1 M PBS (pH 7.4). The decay curves of **2**–**4** were obtained by deducing the concentrations of aglycones **5**–**7** generated by the hydrolysis of the initial concentrations

of **2**–**4**, respectively. Each time the concentrations of **2**–**4** were calculated using calibration curves (Figures S5-S7). The first-order rate constants, k (min^{-1}) were obtained from the decay curves of **2**–**4** calculated using the concentrations of aglycones **5**–**7** measured at intervals of 1, 2, 3, 4, 5, 10, 15, 20, and 25 min after the addition of 20 μL of *β*-galactosidase at 323 K (Figure 6, Table 3).

However, because **3** was associated with a small rate constant, the hydrolysis rate of **3** using 60 μL of *β*-galactosidase in 0.1 M PBS (pH 7.4) was measured.

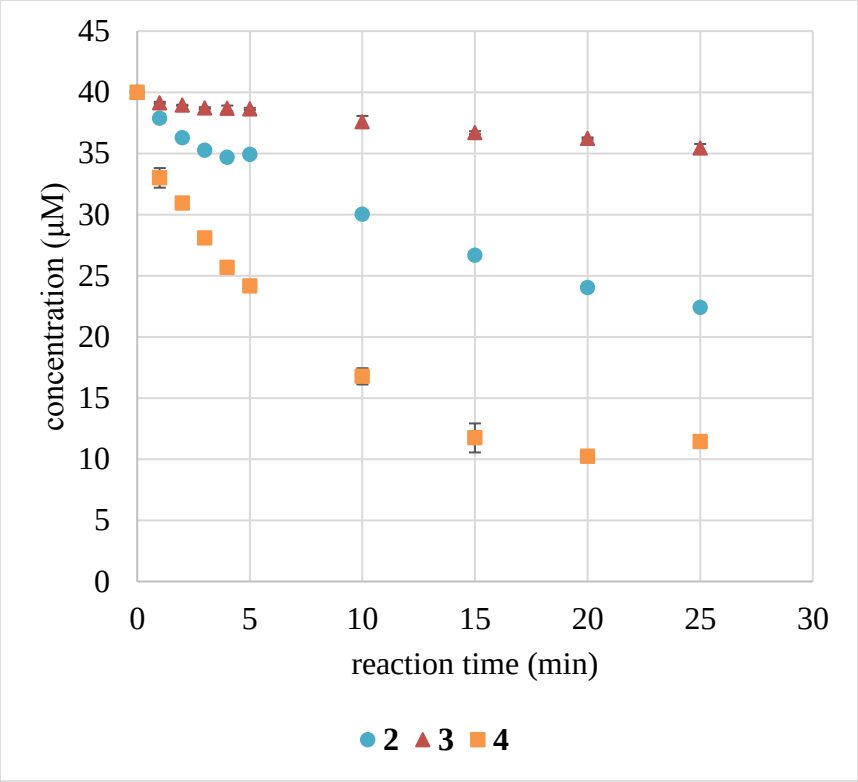

Figure 6. Time-dependent hydrolysis profiles of the three nitroxide *O*-galactosides **2**–**4** with 20 μL *β*-galactosidase in 0.1 M PBS (pH 7.4) at 323 K. Each data represents mean ± S.D., n = 3.

Table 3. Pseudo-first-order rate constants k (min^{-1}) for the initial rates of hydrolysis of the three nitroxide *O*-galactosides **2**–**4** with 20 μL *β*-galactosidase at 323 K, based on the Figure 6. (mean ± S.D., n = 3).

compound	k (min^{-1})	R^2
2	$2.1\times10^{-2} \pm 1.3\times10^{-3}$	0.99
3	$6.6\times10^{-3} \pm 4.5\times10^{-4}$	0.98
4	$0.13 \pm 2.3\times10^{-3}$	0.98

Hydrolysis rate constants *k* (min^{-1}) for initial rates of reduction of TEMPO *O*-galactoside (3) with 60 μL *β*-galactosidase.

The rate of hydrolysis of *O*-galactoside **3** was studied under pseudo-first-order conditions using 60 μL *β*-galactosidase in 0.1 M PBS (pH 7.4). The decay curve and rate constant of **3** were obtained by the above method, yielding a suitable high R^2 (0.99) curve, and a rate constant of 0.042 ± 0.002 min^{-1} (Figure S7, Table S1).

The order of decay due to hydrolysis was **4** > **2** > **3**. The rate constant for **4** was 0.13 ± 2.3×10^{-3} min^{-1} and 6.2 times larger than that for **2** (2.1×10^{-2} ± 1.3×10^{-3}), which was 3.2 times larger than that for **3** (6.6×10^{-3} ± 4.5×10^{-4}). In particular, the hydrolysis rate of **4** was faster compared to **2** and **3**. The order of the measured hydrolysis rates for **2**–**4** was consistent with that expected from the reactivity of the alcohols of **2**–**4**; phenol for **4** > primary alcohol for **2** > secondary alcohol for **3**.

Bioassay

Herein, **4** was selected as a candidate of bioassay because its hydrolysis rate by *β*-galactosidase was the highest and the reduction reactivity for AsA was the second highest. To 4×10^6 cells of HeLa cells in the growth-proliferating logarithmic period, 100 μL of 40 μM **4** was added suspended via pipetting in the growth medium including 20 mM gadopentetic acid (GdDTPA), based on the method established by Bottle et al.[29] This led to the broadening and disappearance of the signal of the nitroxide-radical outer cell. After 5 min, 50 μL of the mixture containing ca. 2×10^6 cells was separated in a quartz EPR tube and characterized via EPR spectroscopy every 5 min for 25 min at 310 K. The EPR measurement of the PC12 cells (normal cells) was also conducted in a similar manner. EPR intensity in the cells at 10 min and 20 min after the addition of **4** to 2×10^6 HeLa cells or PC12 cells is presented in Figure 7. Although the difference between the EPR intensities in the HeLa and PC12 cells was small at 10 min, at 20 min, no EPR intensity was detected in the PC12 cells, whereas that in the HeLa was remained. These results indicate that the more nitroxide-radicals were remained in Hela cells persisted. However, because the detectable EPR intensity in the cells was low, the following can be deduced: 1) the number of cultured cells (2×10^6) is smaller than the number of cancer cells derived from living organisms, 2) **4** is easily reduced in the cells. To increase the EPR intensity, increasing the cultured cells for measurement and introducing more resistant nitroxides for the reduction substance *in vivo* might be required in the spin-label probe. Furthermore, the detailed analysis for this result is needed in the future, because the difference of the redox state between Hela and PC 12 cells is unclear.

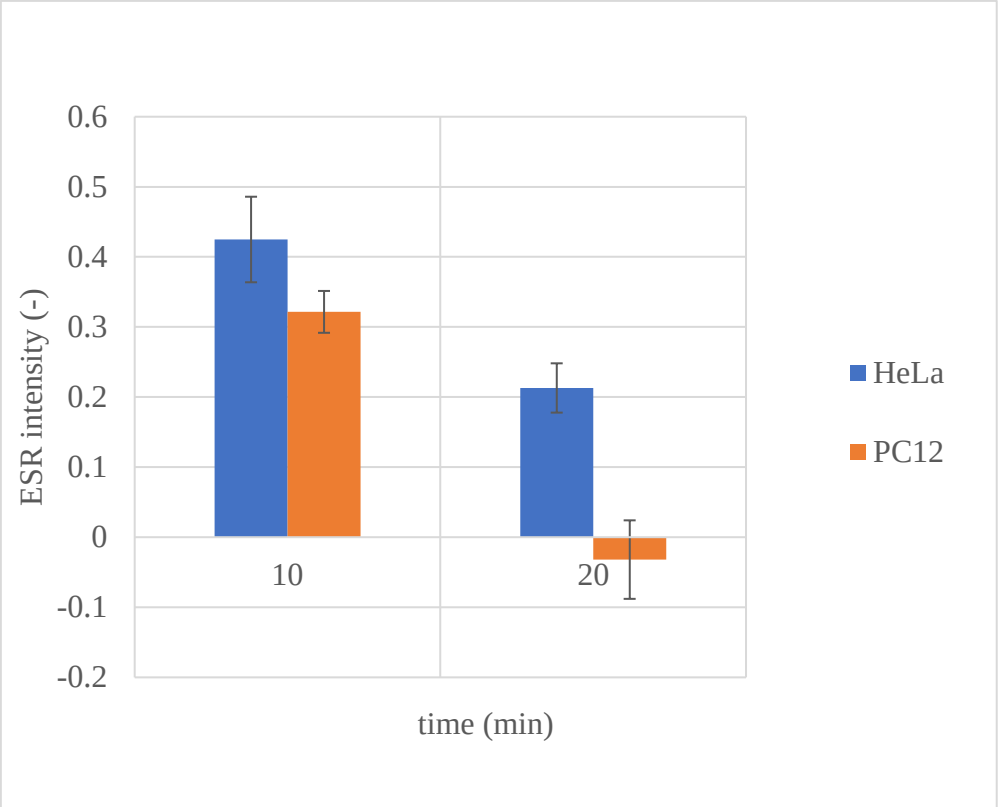

Figure 7. Time-dependent cell localization of **4** with 40 mM GdDTPA in DMEM (No-Gul) at 310 K. Data shown are means ± S.D. of the data from the three experiments ($p < 0.01$).

In conclusion, for three nitroxide-radical *O*-galactosides **2**, **3**, and **4**, two in-vitro screenings were conducted. The reduction reactivity for AsA followed the order: **2** > **4** > **3**. The hydrolysis reactivity for *β*-galactosidase exhibited the order: **4** > **2** > **3**. For a bioassay using HeLa and PC12 cells, we gave priority to the reactivity for *β*-galactosidase according our concept and selected **4**. The EPR intensity in the cancer cells and normal cells after the addition of **4** was measured, indicating the number and life of the radical species remaining in the cells. It was found that the radical species (**4** and/or its aglycone-nitroxide **7**) persisted longer in the HeLa cells than in the PC 12 cells: however, the radical intensity in the former was low. If a spin label selectively incorporated into cancer cells is developed, cancer cells may be visualized non-invasively by the techniques merged EPR and magnetic resonance imaging (MRI) in the future.[13]

EXPERIMENTAL

Synthesis

Materials and apparatus All the starting materials and reagents were purchased from FujifilmWako, Japan and Sigma-Aldrich, USA. The reactions were monitored via thin-layer chromatography (TLC) on 0.25-mm silica gel F254 plates (E. Merck). A 7% ethanolic solution of phosphomolybdic acid with

heating was used for coloration. Flash column chromatography was performed on silica gel (silica-gel 60, 40–50 μm, Kanto Chemical Co. Inc., Japan) to separate and purify the reaction products. Optical rotations were recorded on a JASCO DIP-370 polarimeter. NMR spectra were recorded on a JEOL ECX-500 spectrometer using Me_4Si as the internal standard. High-resolution mass spectrometry (HRMS) was conducted under electron spray ionization (ESI) conditions on a JEOL JMS-T100LP.

EPR analysis EPR spectra were obtained using a JEOL JES-FR30 EPR spectrometer. The samples were drawn into quartz capillaries. The bottoms of the capillaries were sealed, and they were placed in standard quartz EPR tubes (outside-diameter: 1.95–1.65 mm, Terumo Co., Japan). The EPR spectrometer settings were as follows: microwave power, 4.0 mW; frequency, 9.5 GHz; and, modulation amplitude, 1.25 G.

***O*-*β*-D-Galactosyl-3-hydroxymethyl-2,2,5,5-tetramethylpyrrolidine-1-oxyl (*O*-*β*-D-galactosyl PROXYL 2).**

To a stirred solution of **5** (110 mg, 0.64 mmol) and per-*O*-benzoyl-α-D-galactosyl bromide (637 mg, 1.5 eq.) in CH_2Cl_2 (2 mL), molecular sieves (MA) 4Å powder (0.5 g) and AgOTf (248 mg, 1.5 eq.) were added dropwise at 0 °C under Ar atmosphere. The resultant mixture was stirred in dark at 25 °C for 18 h. The reaction mixture was filtered through a Celite® pad. The filtrate was washed with saturated $NaHCO_3$ (aq., 5mL) and then dried over anhydrous $MgSO_4$. Following removal of the organic solvent by evaporation, the residue was separated by silica-gel column chromatography (2;1 1-hexane:AcOEt) to afford *O*-*β*-galactoside (84 mg, 26%), which was dissolved in dry MeOH (5 mL). To this stirred mixture, 25% NaOMe in MeOH solution (0.7 mL) was added dropwise. After 0.5 h, to the reaction mixture, Dowex 50W × 8 (H^+) resin was added until the resultant mixture was neutralized, which was subsequently filtered and washed with MeOH. Following evaporation, the residue was purified by silica-gel column chromatography (5:1 $CHCl_3$:MeOH), yielding **2** (54 mg, 97.3%) as a pale-yellow powder.

Pale-yellow powder; R_f 0.28 (5:1 $CHCl_3$:MeOH); ESI-MS (*m*/*z*) 357 $(M+Na)^+$; HRMS calcd for $C_{15}H_{28}NNaO_7$ $[M+Na]^+$ 357.1764, found 357.1776. X-band EPR data: g = 2.007, aN = 1.63 mT (Figure S8).

3-*O*-(2′,3′,4′,6′-Tetra-*O*-acetyl-*β*-D-galactosyl)-3-hydroxymethyl-*N*-acetoxytetramethylpyrrolidine (2′). To a stirred solution of **2** (44.2 mg, 0.13 mmol) in EtOH (1.5 mL), hydrazine monohydrate (0.5 mL) was added, and the mixture was stirred at 25 °C for 1 h. Following confirmation of the completion of the reaction by silica-gel TLC, the solvent was removed by evaporation, and the residue was dissolved in acetic anhydride (0.5 mL) and pyridine (0.25 mL) and the mixture was stirred at 25 °C for 18 h. To the reaction mixture, ice-cold water (10 mL) was added, and it was extracted twice with AcOEt. Following

evaporation, the residue was purified by silica-gel chromatography ($CHCl_3$), yielding **2′** (57.7 mg, 80.0%) as a white powder. White powder; R_f 0.30 (1-Hexane:AcOEt=3:2); $[\alpha]_D^{21}$ -9.2 (*c* 0.414, $CHCl_3$); ^{1}H NMR ($CDCl_3$) δ 1. 042, 1.159, 1.148, and 1.190 (br.s, 12H, br.s, Me x 4), 1.55 (1H, br.t, *J* = 11.9 Hz, H3), 1.81 (1H, dd, *J* = 7.3 and 11.9 Hz, H3), 2.28 (1H, br.m, H2), 3.38 (0.5H, br.t, *J* = 9.2 Hz, 3-CH_2), 3.47 (0.5H, t, *J* = 9.2 Hz, 3-CH_2), 3.90 (0.5H, br.t, 3-CH_2), 3.97 (0.5H, Br.t, 3-CH_2), 2.033 and 2.042 (each 1.5H, s, NOAc), (galactose moiety) 3.90 (1H, t, *J* = 6.4 and 8.3 Hz, H5′), 4.12 (1H, dd, *J* = 8.3 and 11.0 Hz, H6′a), 4.19 (1H, dd, *J* = 6.4 and 11.0 Hz, H6′b), 4.45 (1H, d, *J* = 7.3 Hz, H1′), 5.00 (1H, dd, *J* = 2.7 and 10.1 Hz, H3′), 5.20 (1H, dd, *J* = 8.3 and 10.1 Hz, H2′), 5.39 (1H, d, *J* = 2.3 Hz, H4′), 1.987, 2.053, 2.103, 2.157 (each s, 3H, OAc x 4); ^{13}C NMR ($CDCl_3$) δ 171.197, 170.411, 170.277, 170.182, and 169.262 (OAc x 5), 20.758 (3C, OAc), 20.672 (6C, OAc x 2), 20.576 (3C, OAc), 19.178 (3C, OAc), (galactose moiety) 101.473 and 101.119 (each 0.5C, C1′), 70.920 and 70.863 (each 0.5C, C2′), 70.633 and 70.614 (each 0.5C, C3′), 36.766 and 68.727 (each 0.5C, C4′), 66.975 (1C, C5′), 61.163 (1C, C6′). HRMS calcd for $C_{25}H_{39}NNaO_{12}$ $[M+Na]^+$ 568.2370, found 568.2370.

4-*O*-(*β*-D-Galactosyl-2,2,6,6-tetramethylpiperidine-1-oxyl (4-*O*-*β*-D-galactosyl TEMPO 3). To a stirred mixture of 4-hydroxy-TEMPO (172 mg, 1 mmol), per-*O*-acetylglucosyl α-fluoride (223 mg, 1.2 mmol), and MS 4 Å (220 mg) in dry CH_2Cl_2 (3.0 mL), $BF_3{\cdot}OEt_2$ (301 μL, 2.4 mmol) was added at 0 °C, and the mixture was stirred 25 °C for 6 h under Ar atmosphere. The reaction mixture was quenched with cold water and filtered through a Celite® pad. The filtrate was extracted with AcOEt thrice. The extract was washed with brine and dried over anhydrous Na_2SO_4. The organic solvent was removed under reduced pressure. The residual syrup was separated and purified by silica-gel column chromatography (2:1 1-hexane:AcOEt, then 20:1 $CHCl_3$:MeOH) to produce the α-anomer (88 mg, 17.5%) as a reddish viscous oil and the β-anomer (117 mg, 23.4%) as a pale-red solid. The β-anomer (117 mg) was de-*O*-acetylated by the same method for **2** to yield **3** (78 mg, 100%). Pale-yellow powder; R_f 0.47 (5:1 $CHCl_3$:MeOH); HRMS calcd for $C_{15}H_{28}NNaO_7$ $[M+Na]^+$ 357.1763, found 357.1744; X-band EPR data *g* = 2.007, aN = 1.71 mT (Figure S9).

4-*O*-(2′,3′,4′,6′-Tetra-*O*-acetyl-*β*-D-galactosyl)-2,2,6,6-tetramethyl-*N*-acetoxypiperidine (3′). Acetate of **3** (**3′**) was synthesized with 94.8% yield by the same method used for the synthesis of **2′**. White powder; R_f 0.42 (3:2 1-Hexane:AcOEt); $[\alpha]_D^{21}$ -18.6 (*c* 0.549, $CHCl_3$);^{1}H NMR ($CDCl_3$) δ 1. 037, 1.018, 1.129, and 1.135 (each s, Me x 4), 1.565 and 1.728 (each 1H, br.t, *J* = 11.9 Hz, H3a), 1.80 and 1.88 (each 1H, br.dt, *J* = 11.9 Hz, H3b), 3.93 (1H, m, H4), (galactose moiety) 3.85 (1H, t, *J* = 6.4 Hz, H5′), 4.05 (1H, dd, *J* = 6.4 and 11.0 Hz, H6′a), 4.14 (1H, dd, *J* = 6.5 and 11.0 Hz, H6′b), 4.49 (1H, d, *J* = 8.4 Hz, H1′), 4.95 (1H, dd, *J* = 2.8 and 10.0 Hz, H3′), 5.09 (1H, dd, *J* = 8.4 and 10.0 Hz, H2′), 5.32 (1H, d, *J* = 2.8 Hz, H4′), 1.918, 1.976, 1.979, 2.031, 2.083 (each s, 3H, OAc x 5); ^{13}C NMR ($CDCl_3$) δ: 170.459, 170.239,

170.153, 170.048, and 169.052 (OAc x 5), 70.240 (C4), 44.877 and 43.622 (C3), 59.852 and 60.005 (C2), 99.156 (C1′), 70.767 (C2′), 70.499 (C3′), 68.718 (C4′), 66.860 (C5′), 61.182 (C6′), 20.614 (OAc), 20.538 (OAc x 2), 20.161 (OAc), 18.919 (NOAc); HRMS calcd for $C_{25}H_{39}NNaO_{12}$ $[M+Na]^+$ 568.2370, found 568.2371.

5-*O*-*β*-D-Galactosyl-1,1,3,3-tetramethyl-5-hydroxylisoindoline-2-oxyl (5-*O*-*β*-D-galactosyl HTMIO 4). To a solution of **7** (72 mg, 0.35 mmol) in quinoline (0.5 mL), Ag_2CO_3 (193 mg, 0.70 mmol) and per-*O*-acetylglucosyl α-bromide (288 mg, 0.70 mmol) were added at 0 °C, and the resultant mixture was stirred at 25 °C in dark under Ar atmosphere for 3 h. The reaction was quenched with MeOH, and the mixture was eluted through a short silica-gel column with AcOEt. The eluate was evaporated to dryness. To the residue, 1 M HCl (8 mL) was added, and the resultant mixture was extracted thrice with AcOEt. The organic layer was washed with water and brine, and subsequently dried over anhydrous Na_2SO_4. Following evaporation, the residue was purified by silica-del column chromatography ($CHCl_3$) to afford the desired *O*-*β*-galactoside (80 mg), which was de-*O*-acetylated similarly to **2** to produce **4** (54 mg, 42%) as a pale-yellow powder. Pale-yellow powder; R_f 0.30 (10:1 $CHCl_3$:MeOH); HRMS calcd for $C_{18}H_{26}NNaO_7$ $[M+Na]^+$ 391.1607, found 391.1612; X-band EPR data g = 2.008, aN = 1.59 mT (Figure S10).

5-*O*-(2′,3′,4′,6′-Tetra-*O*-acetyl-*β*-D-galactosyl)tetramethyl-5-hydroxyl-*N*-acetoxyisoindoline (4′). Acetate of **4** (**4′**) was synthesized with 91.8% yield by the same method used for the synthesis of **2′**. White powder; R_f 0.29 (3:2 1-Hexane:AcOEt); $[\alpha]_D^{21}$ +6.9 (*c* 0.519, $CHCl_3$); ^{1}H NMR ($CDCl_3$) δ 1. 378 and 1.468 (each s, 6H, Me x 4), 6.77 (1H, br.d, J = 1.8 Hz, H6), 6.91 (1H, dd, J = 1.8 and 8.3 Hz, H4), 7.05 (1H, d, J = 8.3 Hz, H3), (galactose moiety) 4.07 (1H, t, J = 6.4 Hz, H5′), 4.17 (1H, dd, J = 6.4 and 11.0 Hz, H6′a), 4.22 (1H, dd, J = 6.4 and 11.0 Hz, H6′b), 5.05 (1H, d, J = 8.3 Hz, H1′), 5.12 (1H, dd, J = 8.3 and 10.3 Hz, H2′), 5.49 (1H, dd, J = 2.8 and 10.1 Hz, H3′), 5.47 (1H, d, J = 2.8 Hz, H4′), 2.027, 2.067, 2.091, 2.197, 2.209 (each s, 3H, OAc x 5); ^{13}C NMR ($CDCl_3$) δ 171.503, 170.335, 170.201, 170.095, 169.387 (OAC x 5), 156.691, 145.512, 122.614, 116.343 and 116.209 (each 0.5C), 110.560, 68.095, 67.866, 28.896, 28.714, 25.315, 25.172 (each br.s, CH_3 x 4), 20.739, 20.624 (C x 2), 20.547, 19.202 (OAc x 5), (galactose moiety) 99.730, 71.025, 70.748, 68.627, 66.894, 61.532; HRMS calcd for $C_{28}H_{37}NNaO_{12}$ $[M+Na]^+$ 602.2213, found 602.2240.

Analysis

Reagents The reagents used in this study were commercial products: L-ascorbic acid (FujifilmWako, Japan), *β*-galactosidase (from Escherichia, >500 units/mg protein, Sigma-Aldrich, USA), and GdDTPA (Sigma-Aldrich, USA).

Reduction of 2-4 using AsA

Apparatus EPR spectra were obtained using a JEOL JES-FR30 EPR spectrometer. The samples were drawn into quartz capillaries, the bottoms of the capillaries were sealed, and the capillaries were placed in standard quartz EPR tubes (outside-diameter: 1.95–1.65 mm, Terumo Co., Japan). The EPR spectrometer settings were as follows: microwave power, 4.0 mW; frequency, 9.5 GHz; and modulation amplitude, 1.25 G.

EPR analysis Following deoxygenation by microwave under reduced pressure, 0.1 M PBS was used for the EPR analysis. To 40 μL of each 40 μM solution of **2**–**4** in 0.1 M PBS (pH 7.4), 40 μL of 2 mM AsA in 0.1 M PBS (pH 7.4) was added, and the mixture was stirred at 295 K for 30 sec. The reaction mixture was collected every 1 min for 20 min after 1 min and subjected to EPR analysis.

Hydrolysis of 2, 3, and 4 using *β*-galactosidase

Apparatus The mixing of the sample was conducted using an AS ONE ASCM-1 shaking agitator. The HPLC analysis was performed using a Silica Pak column (silica gel, 5 μm, 4.6 × 150 mm, Shodex®, Japan).

HPLC analysis The hydrolysis of the *O*-*β*-galactosides **2**–**4** by *β*-galactosidase was monitored via HPLC. Because in the reaction mixture, **2**–**4** were inseparable in HPLC, the concentrations of their aglycones, **5**–**7** generated by hydrolysis (i.e. those of **2**–**4** reacted) were measured. Moreover, the decay of each concentration of **2**–**4** was determined by deducing each concentration of **5**–**7** generated hourly from each initial concentration of **2**–**4**. To each 40 μM solution (4 mL) of **2**–**4** in 0.1 M PBS (pH 7.0) warmed at 50 °C, 10 μL of *β*-galactosidase was added, and the reaction was started. Using a micropipette, 400 μL of the reaction mixture was collected at 1, 2, 3, 4, 5, 10, 15, 20, and 25 min and then extracted with 200 μL of $CHCl_3$ similar to the mentioned below. Using a microsyringe, exactly 10 μL of the $CHCl_3$ extract was subjected to the HPLC analysis.

HPLC conditions The HPLC conditions were column: silica-gel and flow rate: 1 mL/min. For **2**, mobile phase: $CHCl_3$:MeOH (95:5), detection: UV 254 nm, and t_R of **5** = 3.592 min (Figure S1). For **3**: mobile phase: $CHCl_3$:MeOH = 98:2, detection: UV 254 nm, t_R of **6** = 4.453 min (Figure S2). For **4**, mobile phase: $CHCl_3$, detection: UV 270 nm, and t_R of **7** = 8.223 min (Figure S3).

Calibration curve Each 50 μM solution of **5**–**7** in PBS was diluted twice with 2 mL of PBS containing 10 μL of *β*-galactosidase to form 50, 25, 12.5, 6.25, 3.13, 1.56, and 0.781 μM solutions. 400 μL of each concentration was extracted with 200 μL of $CHCl_3$, which was stirred by a shaking agitator (2000 rpm × 30 min) and the kept standing for 1 h. Moreover, precisely 10 μL of the lower $CHCl_3$ layer was obtained using a microsyringe and thereafter subjected to HPLC analysis. The calibration curves of the peak areas

of the HPLC versus the concentrations of each **5**–**7** were prepared (Figures S4–S6).

Cell Culture

HeLa cells acquired from RIKEN Bio-Resource Center (Tsukuba, Japan) were cultured in DMEM (043-30085; FujifilmWako, Japan) supplemented with 10% fetal bovine serum and 1% (w/v) streptomycin/penicillin solution (26253-84, Nacalai Tesque, Japan) in the presence of 5% CO_2 in air at 37 °C. A 100-mL aliquot of HeLa cells (5000 cells/mL) was added to Φ 90-mm dishes (TR5003; True Line, USA) and incubated. Culture medium including HeLa cells of logarithmic growth phase in a dish (Φ 90 mm) was washed twice with 3 mL of PBS, and then with 3 mL of 2.5g/L-trypsin/1 mM/L-EDTA. To the remained HeLa cells 0.5 mL in 2.5g/L-trypsin/1 mM/L-EDTA was added and incubated under 5% CO_2 at 37 °C for 5 min, to which 2.5 mL of growth medium was added and pipetting. 1 mL of the resulting suspension was splitted to three dishes (Φ 90 mm) including 12 mL of growth medium, respectively. The resulting medium was incubated under 5% CO_2 at 37 °C, and then subjected to bioassay.

Bioassay

The intracellular concentrations of the nitroxides were determined by comparing the EPR signal intensities with/without the broadening agent. Briefly, each nitroxide (0.2 mM) was added to a cell suspension containing 1×10^6 HeLa or PC12 cells/50 μL, and the EPR spectra were measured at 10 min and 20 min time points using an X-band EPR spectrometer. The suspension was kept in an incubator to maintain the cell viability during the experiments. An extracellular broadening agent, GdDTPA (20 μL) was added to broaden the EPR signals of the extracellular nitroxide present in the cell suspension. The final concentration of the broadening agent was 20 mM. The remaining EPR signal provides a direct measure of the nitroxide localized in the intracellular compartments of the HeLa or PC12 cells.

CONFLICT OF INTEREST

The authors have declared that there is no conflict of interest.

REFERENCES

1. H. Kobayashi, M. Ogawa, R. Alford, P. L. Choyke, and Y. Urano, *Chem. Rev*., 2010, **110**, 2620.
2. R. N. Dsouza, U. Pischel, and W. M. Nau, *Chem. Rev.*, 2011, **111**, 7941.
3. X. Chen, T. Pradhan, F. Wang, J. S. Kim, and J. Yoon, *Chem. Rev.*, 2012, **112**, 1910.
4. D. Asanuma, M. Sakabe, M. Kamiya, K. Yamamoto, J. Hiratake, M. Ogawa, N. Kosaka, P. L. Choyke, T. Nagano, H. Kobayashi, and Y. Urano, *Nature Commun.*, 2015, **6463**. DOI:

10.1038/ncomms7463.

5. M. Kamiya, D. Asanuma, E. Kuranaga, A. Takeishi, M. Sakabe, M. Miura, T. Nagano, and Y. Urano, *J. Am. Chem. Soc.*, 2011, **133**, 12960.
6. F. Hyodo, K. H. Chuang, A. G. Goloshevsky, A. Sulima, G. L. Griffiths, J. B. Mitchell, A. P. Koretsky, M. C. Krishna, and J. Cereb, *Blood Flow Metab.*, 2008, **28**, 1165.
7. M. Yamato, T. Shiba, K. Yamada, T. Watanabe, H. Utsumi, and J. Cereb, *Blood Flow Metab.*, 2009, **29**, 1655.
8. H. Fujii, H. Sato-Akaba, K. Kawanishi, and H. Hirata, *Magn. Reson. Med.*, 2011, **65**, 295.
9. A. Matsumura, M. C. Emoto, S. Suzuki, N. Iwahara, S. Hisahara, J. Kawamata, H. Suzuki, A. Yamauchi, H. Sato-Akaba, H. G. Fujii, and S. Shimohara, *Free Radic. Biol. Med.*, 2015, **85**, 165.
10. S. Sato, M. Yamaguchi, A. Nagai, R. Onuma, M. Saito, R. Sugawara, S. Shinohara, E. Okabe, T. Ito, and T. Ogata, *Spectrochim. Acta Part A*, 2014, **124**, 322.
11. S. Sato, M. Suzuki, T. Soma, and M. Tsunoda, *Spectrochim. Acta Part A*, 2008, **70**, 799.
12. S. Sato, M. Tsunoda, M. Suzuki, M. Kutsuna, K. Takido-uchi, M. Shindo, H. Mizuguchi, H. Obara, and H. Ohya, *Spectrochim. Acta Part A*, 2009, **71**, 2030.
13. M. C. Emoto, S. Sato, and H. G. Fujii, *Magn. Reson. Chem.*, 2016, **54**, 705.
14. K. Sasaki, T. Ito, H. G. Fujii, and S. Sato, *Chem. Pharm. Bull.*, 2016, **64**, 1509.
15. M. C. Emoto, K. Sasaki, K. Maeda, H. G. Fujii, and S. Sato, *Chem. Pharm. Bull.*, 2018, **66**, 887.
16. K. Thomas, T. W. Moody, R. T. Jensen, J. Tong, C. L. Rayner, N. L. Barnett, K. E. Fairfull-Smith, L. A. Ridnour, D. A. Wink, and S. E. Bottle, *Eur. J. Med. Chem.*, 2018, **147**, 34.
17. S. Sato, T. Kumazawa, S. Matsuba, J. Onodera, M. Aoyama, H. Obara, and H. Kamada, *Carbohydr. Res.*, 2001, **334**, 215.
18. E. G. Rozantsev, "In Free Nitroxyl Radicals," ed. by H. Ulrich, Plenum Press, New York, 1970, pp. 203-246.
19. "Spin Labeling, Theory and Application", ed. by L. J. Berliner, Academic Press, Inc., 1976.
20. B. Hatano, H. Araya, Y. Yoshimura, H. Sato, T. Ito, T. Ogata, and T. Kijima, *Heterocycles*, 2010, **81**, 349.
21. P. G. Griffiths, G. Moad, E. Rizzard, and D. H. Solomon, *Aust. J. Chem.*, 1983, **36**, 397.
22. D. J. Keddie, T. E. Johnson, D. P. Arnold, and S. E. Bottle, *Org. Biomol. Chem.*, 2005, **3**, 2593.
23. A. G. M. Barrett, G. R. Hanson, A. J. P. White, D. J. Williams, and A. S. Micallef, *Tetrahedron*, 2007, **63**, 5244.
24. J. P. Blinco, J. L. Hodgson, B. J. Morrow, J. R. Walker, G. D. Will, M. L. Coote, and S. E. Bottle, *J. Org. Chem.*, 2008, **73**, 6763.
25. V. C. Lussini, J. P. Blinco, K. E. Fairfull-Smith, and S. E. Bottle, *Chem. Eur. J.*, 2015, **21**, 18258.

26. K. Oyama and T. Kondo, *Org. Lett.*, 2003, **5**, 209.
27. K. Oyama and T. Kondo, *Tetrahedron*, 2004, **60**, 2025.
28. K. Misawa, Y. Takahashi, and S. Sato, *Chem. Pharm. Bull.*, 2013, **61**, 776.
29. N. Khan, J. P. Blinco, S. E. Bottle, K. Hosokawa, H. M. Swartz, and A. S. Micallef, *J. Magn. Reson.*, 2011, **211**, 170.